In search of a unifying theory of white matter aging: tract perfusion-microstructure relationships

Tyler D. Robinson[1], Yutong L. Sun[1], Paul T. H. Chang[1], J. Jean Chen[1,2,3]

1. Rotman Research Institute, Baycrest, Canada
2. Medical Biophysics, University of Toronto, Canada
3. Biomedical Engineering, University of Toronto, Canada

ABSTRACT

Age-related degeneration of white matter (WM) tissue in the brain has been found to underlie progressive cognitive declines in healthy populations. Understanding and predicting these changes is necessary to building a more unified model of the aging brain and improving interventions. We posit that regional hypoperfusion in the WM precedes deteriorating WM integrity, as evidenced by studies demonstrating relationships between declining cortical perfusion and the development of WM hyperintensities. This remains an understudied area of WM aging, in part due to technical challenges in quantifying WM perfusion. This study seeks to examine tract-wise associations between WM microstructural integrity and perfusion parameters in the Human Connectome Project - Aging (HCP-A) participants. Perfusion was measured by cerebral blood flow (CBF) and arterial transit time (ATT), while microstructural integrity was measured by fractional anisotropy (FA), mean diffusivity (MD), axial diffusivity (AD), and radial diffusivity (RD). Their associations are assessed in ten major bilateral WM tracts. Results show that WM perfusion-microstructure relationships vary both by tract and by sex. We identify consistent patterns of associations between perfusion and microstructure that suggest the presence of multiple distinct stages of deterioration, with female subjects demonstrating more tracts in advanced stages of decline. Additionally, ATT appears to be the earliest indicator of WM declines, preceding age-related differences in WM microstructure in several tracts. This study contributes compelling evidence to the vascular hypothesis of WM degeneration, and highlights the utility of blood-flow timing rather than CBF as an early marker of aging.

INTRODUCTION

Increasing understanding of the importance of neurovascular health in maintaining tissue integrity has led to the examination of tissue structure-perfusion associations in brain aging. The current literature focuses largely on gray matter (GM) perfusion and its associations with cortical and subcortical atrophy (Baker et al., 2014; Chen et al., 2011, 2013; C.-M. Kim et al., 2020; Mayer et al., 2021). Relationships have been demonstrated between cortical perfusion and cognitive performance (D. Kim et al., 2021), and decreased cortical perfusion may predict heightened vulnerability to pathological declines (Chen et al., 2013; Mayer et al., 2021; O'Sullivan et al., 2002). However, regional variation in age-related cortical atrophy does not appear to match regional reductions in cerebral blood flow (CBF) (Chen et al., 2011). Furthermore, such investigations are scarce in the WM. A well-established relationship between cortical perfusion and the development of WM hyperintensities in associated subcortical regions illustrates the importance of CBF to maintaining the integrity of WM fibers (Bernbaum et al., 2015; O'Sullivan et al., 2002). Recent investigation of tractwise relationships between WM integrity and tract morphometry suggest that microstructural changes are also broadly associated with morphometric declines with age (Robinson et al., 2023). These findings cumulatively suggest that a more complete understanding of the interrelations between perfusion and integrity in both GM and WM is required to achieve a more consistent understanding of brain aging. Although WM microstructure as an earlier indicator of tissue degeneration should associate more directly with WM perfusion than with morphology, the structural-perfusion relationship in the aging WM has not been examined, largely due to challenges in WM perfusion quantification (Bernbaum et al., 2015; Chen et al., 2013). By incorporating regional perfusion measures into ongoing models of WM microstructural and morphometric declines with age, we aim to build a more comprehensive understanding of the mechanics of WM decline and improve early detection of pathological WM changes.

WM microstructural declines in aging are reported in a robust body of literature, demonstrating regional differences in age-related microstructural declines along both broad regional and tract-specific segmentations (Baker et al., 2014; Bender et al., 2016; de Groot et al., 2015, 2016; Sala et al., 2012; Slater et al., 2019). To some extent, patterns of WM decline and resilience appear to broadly follow developmental trajectories (Hoagey et al., 2019; Slater et al., 2019; Stricker et al., 2009). However, due to the limited imaging exploration of WM perfusion, there is limited understanding of regional variation in WM perfusion metrics and how they relate to microstructural declines locally. Nonetheless, one potential hypothesis for these patterns of WM degeneration is that those tracts or regions that demonstrate greater robustness to age-related declines are differentiated from more susceptible regions by differences in

underlying vascular development and decline. Unlike the cortical surface, which is fed by larger vessels along the cortical surface, blood supply to the WM is fed primarily by smaller vessels penetrating into WM tissue from either the cortical surface or the midbrain (Nonaka et al., 2003; Smirnov et al., 2021). This results in both (1) considerable variation in proximity to major vessels and number of blood flow sources and (2) the likelihood that vascular disease and age-related deterioration that differentially affects small vessels has an earlier impact on the WM than on the cortical surface (Akashi et al., 2017; Hase et al., 2018). Tractwise heterogeneity in blood vessel development may then underlie susceptibility to age-related changes in perfusion and regional ability to support continued microstructural integrity with age.

Vascular declines with age have been consistently demonstrated in the WM as part of general systemic vascular decline (Kohn et al., 2015; Li et al., 2018; Tomoto et al., 2023). Increasing arterial stiffness due to the progressive decay of elastin in normal aging results in more fragile blood vessels (Kohn et al., 2015; Tomoto et al., 2023). Even in intact arterial pathways, changes in vessel morphometry result in more tortuous micro- and meso-vasculature with reduced blood flow (Li et al., 2018). As a result, diminished perfusion into WM tissues is expected in healthy aging. As prior research has demonstrated an association between reduced perfusion in the cortex and the development of WM hyperintensities in related WM regions (Mayer et al., 2021), we posit that changes in perfusion in the WM anticipate declines in WM integrity and ultimately the breakdown of WM tissue. This process likely results from the progressive inability of supporting glial cells to maintain myelin in WM fibers as perfusion declines (Kobayashi et al., 2002; Kohama et al., 2012). Those axons with reduced or malformed myelin sheaths are then more vulnerable to age-related culling of vulnerable WM fibers, and associated WM regions at higher risk of pathological declines (Kohama et al., 2012; Tang et al., 1997). Related to perfusion quantification, vascular response latency has been demonstrated as a more sensitive marker of pathology than response amplitude (D. Kim et al., 2021; McKetton et al., 2019; Nanayakkara et al., 2023), so it remains unclear whether perfusion amplitude or timing is an earlier marker of possible WM degeneration.

Given the previously limited ability to measure regional differences in WM perfusion (Bernbaum et al., 2015; Chen et al., 2013) and a relative sparsity of studies addressing WM vascular-microstructural declines on a tractwise basis (Mayer et al., 2021; Smirnov et al., 2021), this study aims to fill both of these knowledge gaps. This choice was motivated by the understanding that WM tracts represent the meaningful structural units for segmentation of the WM (Baker et al., 2014; Sala et al., 2012; Yeatman et al., 2014) in aging, as well as reflecting functional connections between terminal cortical regions (Nozais et al., 2021). This was an important rationale for the previous studies on the morphometry-microstructural associations in WM aging mentioned earlier. As variance in tractwise perfusion remains underexplored in healthy adults, it represents a natural extension to existing literature and a valuable missing component in

modeling regional WM declines with age and may represent an underlying source of differences in order and rate of tractwise declines. Using the Human Connectome Project Aging (HCP-A) data set (Bookheimer et al., 2019), this study sought to map tractwise age-related variations in WM perfusion, as well as the relationships between tractwise WM integrity and perfusion. Perfusion metrics of interest to this study included cerebral blood flow (CBF) and arterial transit time (ATT) to more comprehensively examine age-related differences in both volume and latency of blood flow to our regions of interest. WM microstructural integrity was quantified using fractional anisotropy (FA), mean diffusivity (MD), axial diffusivity (AD), and radial diffusivity (AD). Microstructural and perfusion metrics were compared across age, as well as between sexes, before their age effects being assessed relative to other metrics. We hypothesized that (1) tract perfusion and microstructure will not decline at the same rate at aging, that is to say that (2) tractwise perfusion changes will be detectable at younger ages than microstructural declines.

METHODS

This study drew five hundred and thirty-five healthy adult subjects (300 female, aged 36-100) from the Human Connectome Project in Aging (HCP-A) dataset (OMB Control# 0925-0667 (Bookheimer et al., 2019; Harms et al., 2018). All subjects were in generally good health and without pathological cognitive impairment (i.e. stroke, clinical dementia). Following manual quality control, thirty-two subjects were excluded from this sample due to MRI artifacts that produced notable errors when generating WM masks. Three additional subjects were excluded as age outliers due to being the only subjects of 100 years of age. Thus, the final sample size was 500 subjects (249 female, aged 36-89).

The study accessed whole-brain T1-weighted structural MRI, diffusion-weighted MRI (dMRI), and multi-delay pseudo-continuous arterial spin labeling (pCASL) measures collected using four Siemens Prisma 3T MRI scanners, with a $(1.5mm)^3$ voxel resolution, MB=4, with 93 directions at $b=1500s/mm^2$. Further imaging parameters for structural, diffusion, and perfusion imaging can be found in (Harms et al., 2018).

Image analysis

dMRI data were corrected for eddy-current and susceptibility-related distortions via EDDY prior to use in tractography analysis. Eighteen major WM tracts were reconstructed from the dMRI data using the Tracts Constrained by Underlying Anatomy (TRACULA) tool in Freesurfer version 7.2.0 (Maffei et al., 2021; Yendiki et al., 2011). FSL's fslmaths function was then used to produce per-subject masks of each WM tract in local space. The eighteen reconstructed tracts were combined bilaterally to produce ten

tracts of interest for analysis: The forceps major (Fmajor), forceps minor (Fminor), anterior thalamic radiation (ATR), Cingulum Angular Bundle (CAB), Cingulate Gyrus (CCG), Corticospinal Tract (CST), Inferior Longitudinal Fasciculus (ILF), Superior Longitudinal Fasciculus Parietal (SLFP), Superior Longitudinal Fasciculus Temporal (SLFT), and the Uncinate Fasciculus (UNC) (Figure 1). Rosner's tests were performed to identify and exclude volume outliers per tract in single tract analyses. The resulting subject counts for these analyses were: Fmajor (N=493), Fminor (N=493), ATR (N=497), CAB (N=490), CCG (N=495), CST (N=491), ILF (N=497), SLFP (N=497), SLFT (N=495), and UNC (N=495).

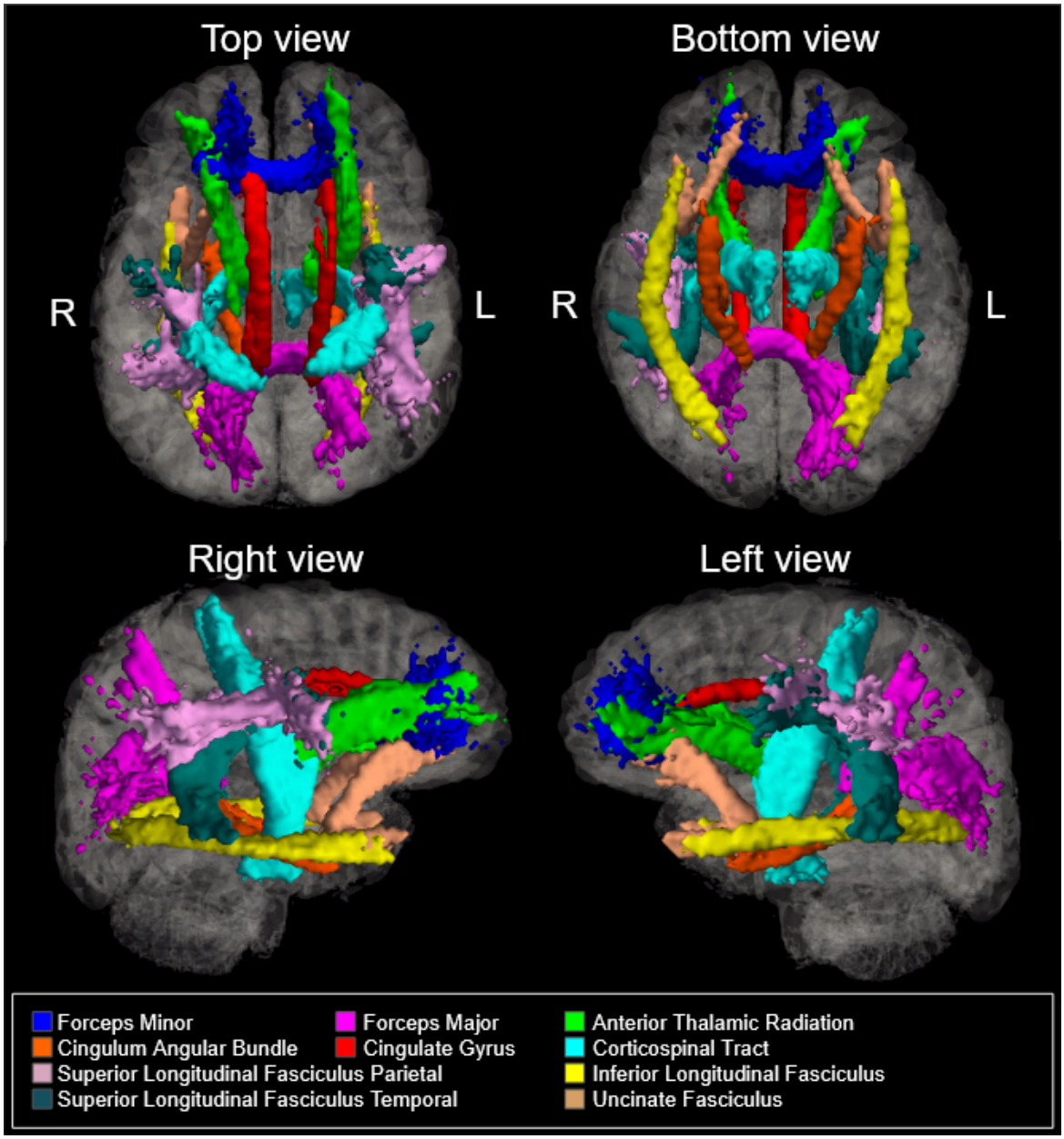

Figure 1: Ten bilateral tracts of interest reconstructed Freesurfer's TRACULA package

Microstructure

FA, MD, AD, and RD maps were derived via Dipy's DKI tool to provide kurtosis-corrected DTI metrics due to the high b-value used in the HCP-A acquisitions. TRACULA generated tract masks were applied to local dMRI images in flsmaths to generate tract means for FA, MD, AD, and RD. For each metric, baseline normalized values ("$FA_{percent}$", "$MD_{percent}$", "$AD_{percent}$", "$RD_{percent}$") were calculated as individual raw tract values divided by the mean raw tract value of the youngest 10% of subjects to assess percent differences from the youngest baseline.

Perfusion

CBF was quantified using the general kinetic model that accounts for arterial-transit delay (FSL oxford_ASL) to produce local CBF and ATT maps. As with microstructure, TRACULA generated tract masks were applied to the local maps in fslmaths to produce tract means for both perfusion metrics. Baseline normalized perfusion values ("$CBF_{percent}$", "$ATT_{percent}$") were again calculated as individual raw tract values divided by the mean raw tract value of the youngest 10% of subjects.

Statistical analysis

Age and sex effects

Between-subjects ANOVA was used to determine the presence of sex differences in tract specific $FA_{percent}$, $MD_{percent}$, $CBF_{percent}$, and $ATT_{percent}$. Whole-WM age-related microstructure and perfusion differences were assessed via multivariate quadratic regression by first regressing age onto mean $FA_{percent}$, $MD_{percent}$,$CBF_{percent}$, and $ATT_{percent}$ values derived from voxel-count weighted tract averages using sex as a covariate of no interest. Subsequent assessment of sex differences in microstructure and perfusion were conducted via sequential multivariate regressions of sex on to mean $FA_{percent}$, $MD_{percent}$, $CBF_{percent}$, and $ATT_{percent}$ using age as a covariate of no interest.

Sequential multivariate regressions were also used to assess tractwise age-related differences in microstructure and perfusion, with age regressed onto $FA_{percent}$, $MD_{percent}$, $CBF_{percent}$, and $ATT_{percent}$ for each of the ten tracts using sex as a covariate of no interest. Sex was subsequently regressed onto $FA_{percent}$, $MD_{percent}$, $CBF_{percent}$, and $ATT_{percent}$ for each of the ten tracts using age as a regressor of no interest. FDR adjustment was again applied to the resulting p-values.

Microstructure vs Perfusion

Two multivariate regression models were constructed to assess relationships between microstructure, perfusion, age, and sex in our sample. Both models were applied first to whole-WM $MD_{percent}$ and $FA_{percent}$ values, then to the individual values for each tract of interest:

- *Model 1. microstructure vs. perfusion across ages:* assesses the degree to which perfusion metrics account for the age-related variability in mean normalized tract MD and FA, with subject sex as a covariate of no interest. That is,
    - $\{FA_{percent}, MD_{percent}\} = f(CBF_{percent}+Sex)$
    - $\{FA_{percent}, MD_{percent}\} = f(ATT_{percent}+Sex)$
- *Model 2. microstructure vs. perfusion between sexes:* assess the degree to which perfusion metrics account for sex-related differences in normalized tract MD and FA, with subject age as a covariate of no interest. That is,
    - $\{FA_{percent}, MD_{percent}\} = f(CBF_{percent}+Age)$
    - $\{FA_{percent}, MD_{percent}\} = f(ATT_{percent}+Age)$
    - One set of models is produced for each sex.

The above analyses were conducted in R (version 4.1.1).

Canonical Correlation Analysis

Canonical correlation analysis (CCA) was conducted to examine the degrees to which each of our variables of interest contributed to age-related differences in microstructure and perfusion respectively. Two column vectors were computed using our perfusion (V_1) variables ($CBF_{percent}$, $ATT_{percent}$) and microstructural (U_1) variables ($AD_{percent}$, $RD_{percent}$, $FA_{percent}$) in Matlab. The linear combinations of V and U vectors which produced the highest correlation were then calculated to determine on a tractwise basis which variables loaded most strongly to age differences by tract. This and following analyses substituted AD and RD variables for the MD variable used in previous analyses as examining the two axes of diffusion separately was more meaningful for clarifying relationships between FA and other diffusion metrics as they relate to microstructural deterioration.

Cross-Correlation Analysis

Cross-correlations functions (CCF) were calculated in Matlab to determine the presence of age-lagged relationships between each measure for perfusion and microstructure. Only variables demonstrating significant non-linear age effects on a tractwise basis were examined in this analysis to reduce ambiguity in CCF interpretation. A curvature threshold for age effects of 0.0005 was implemented. CCFs were calculated based on the models of age effects for six paired tractwise microstructure/morphometry measures, along with cross-comparisons for $AD_{percent}$/$RD_{percent}$ vs $FA_{percent}$ and $CBF_{percent}$ vs $ATT_{percent}$:

- CBF/Microstructure
    - $CBF_{percent}$ vs $AD_{percent}$

  - $CBF_{percent}$ vs $RD_{percent}$
  - $CBF_{percent}$ vs $FA_{percent}$
- ATT/Microstructure
  - $ATT_{percent}$ vs $AD_{percent}$
  - $ATT_{percent}$ vs $RD_{percent}$
  - $ATT_{percent}$ vs $FA_{percent}$
- $AD_{percent}$ vs $FA_{percent}$
- $RD_{percent}$ vs $FA_{percent}$
- $CBF_{percent}$ vs $ATT_{percent}$

RESULTS

Whole-WM analyses

Age differences

A positive relationship with age was identified in $MD_{percent}$ ($F(2, 497) = 78.6$, $p < .001$, $R^2_{Adjusted}$= .24, slope = 0.001 mm^2/s/year) and $ATT_{percent}$ ($F(2, 497) = 10.7$, $p < .001$, $R^2_{Adjusted}$= .04, slope = 0.0002 s/year) when controlling for sex , along with negative relationships with $FA_{percent}$ ($F(2, 497) = 9.77$, $p < .001$, $R^2_{Adjusted}$= .03, slope = -0.0008/year) and $CBF_{percent}$ ($F(2, 497) = 8.40$, $p < .001$, $R^2_{Adjusted}$= .03, slope = -0.003 ml/100g/min/year) We found that a quadratic relationship provided a better fit than a linear model to the age-associations in $CBF_{percent}$, $MD_{percent}$ and $FA_{percent}$, when averaged across all WM tracts (Figure 2).

Sex differences

Following baseline normalization, female subjects demonstrated significantly higher whole-WM $MD_{percent}$ when controlling for age ($F(2, 497) = 78.6$, $p < .001$, $R^2_{Adjusted}$= .24, effect = 0.008 mm^2/s). No significant sex differences were identified in whole-WM $FA_{percent}$, $CBF_{percent}$, or $ATT_{percent}$.

Microstructure-perfusion relationships

Model 1 (perfusion vs microstructure): Significant relationships were identified between $CBF_{percent}$ and $MD_{percent}$ ($F(2, 497) = 5.36$, $p = .005$, $R^2_{Adjusted} = .02$, slope = -0.02), as well as between $ATT_{percent}$ and $MD_{percent}$ ($F(2, 497) = 4.07$, $p = .02$, $R^2_{Adjusted} = .01$, slope = 0.23). No significant whole-WM relationships were found between $FA_{percent}$ and WM perfusion (Table 1a).

Model 2 (sex differences in perfusion-microstructure relationships): No significant relationships were identified between whole-WM microstructure and perfusion in Model 2 (Table 2a).

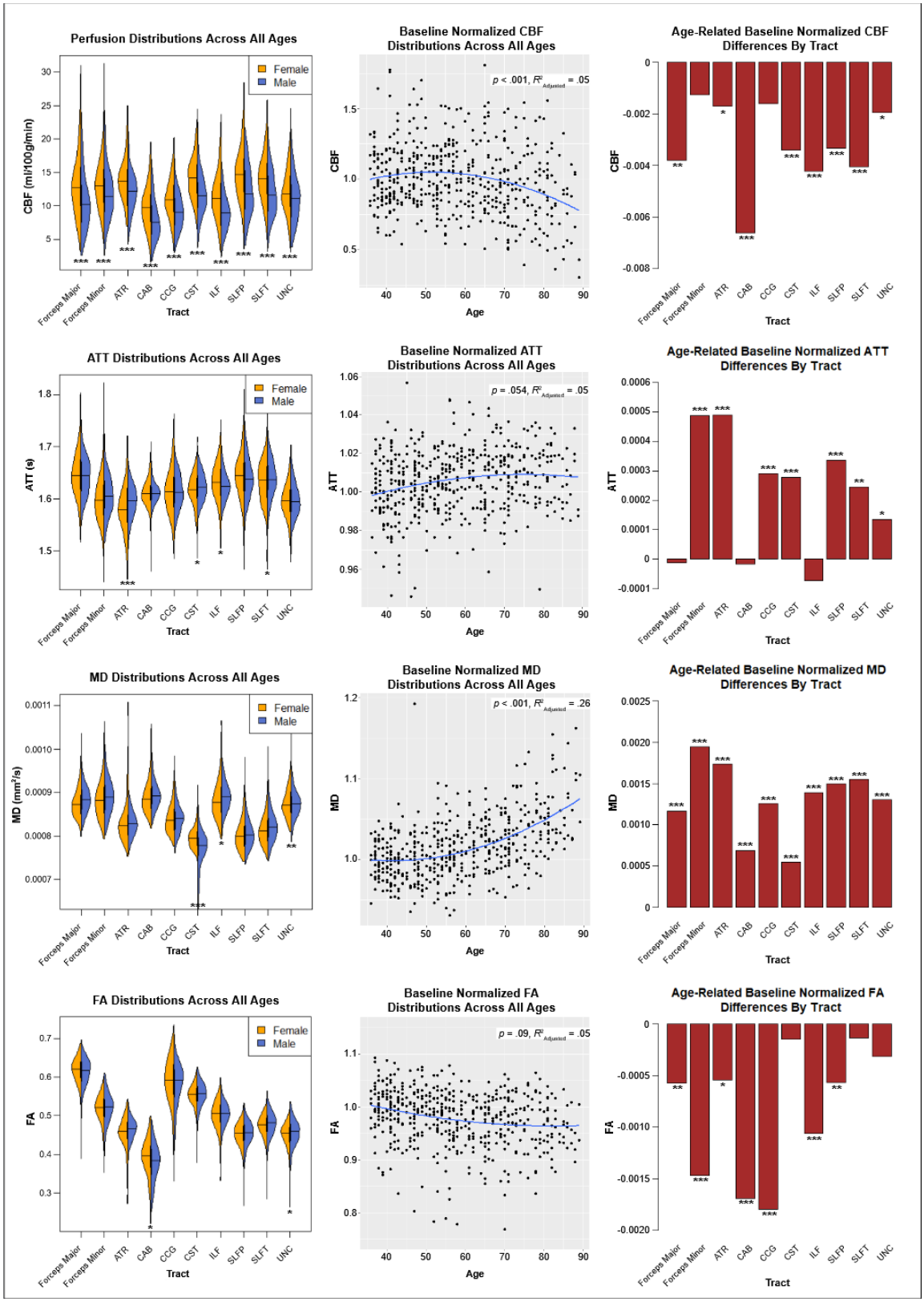

Figure 2: Raw distributions for by sex (left), whole-WM age effects (middle), and tractwise age effects (right) for CBF, ATT, MD, and FA.

Tractwise analyses

Age differences

Significant linear and quadratic relationships between age and $CBF_{percent}$ were identified in all tracts but the UNC, with quadratic regressions providing a better fit in all tracts with the exception of the Fminor and CCG. Significant quadratic effects were identified between age and $ATT_{percent}$ in the Fmajor, ILF, and UNC, along with significant linear effects in the Fminor, ATR, CCG, CST, SLFP, SLFT, and UNC, with quadratic regression providing a better fit in the UNC. Significant linear and quadratic relationships between age and $MD_{percent}$ were identified in all tracts of interest, with quadratic regressions providing a better fit in all tracts. Significant quadratic associations between age and $FA_{percent}$ were found in the Fminor, CCG, and ILF, with significant linear associations in the Fmajor, Fminor, ATR, CAB, CCG, ILF, SLFP. Quadratic regression provided a better fit for the effects of age on FA in the Fminor and CCG (Figure 3).

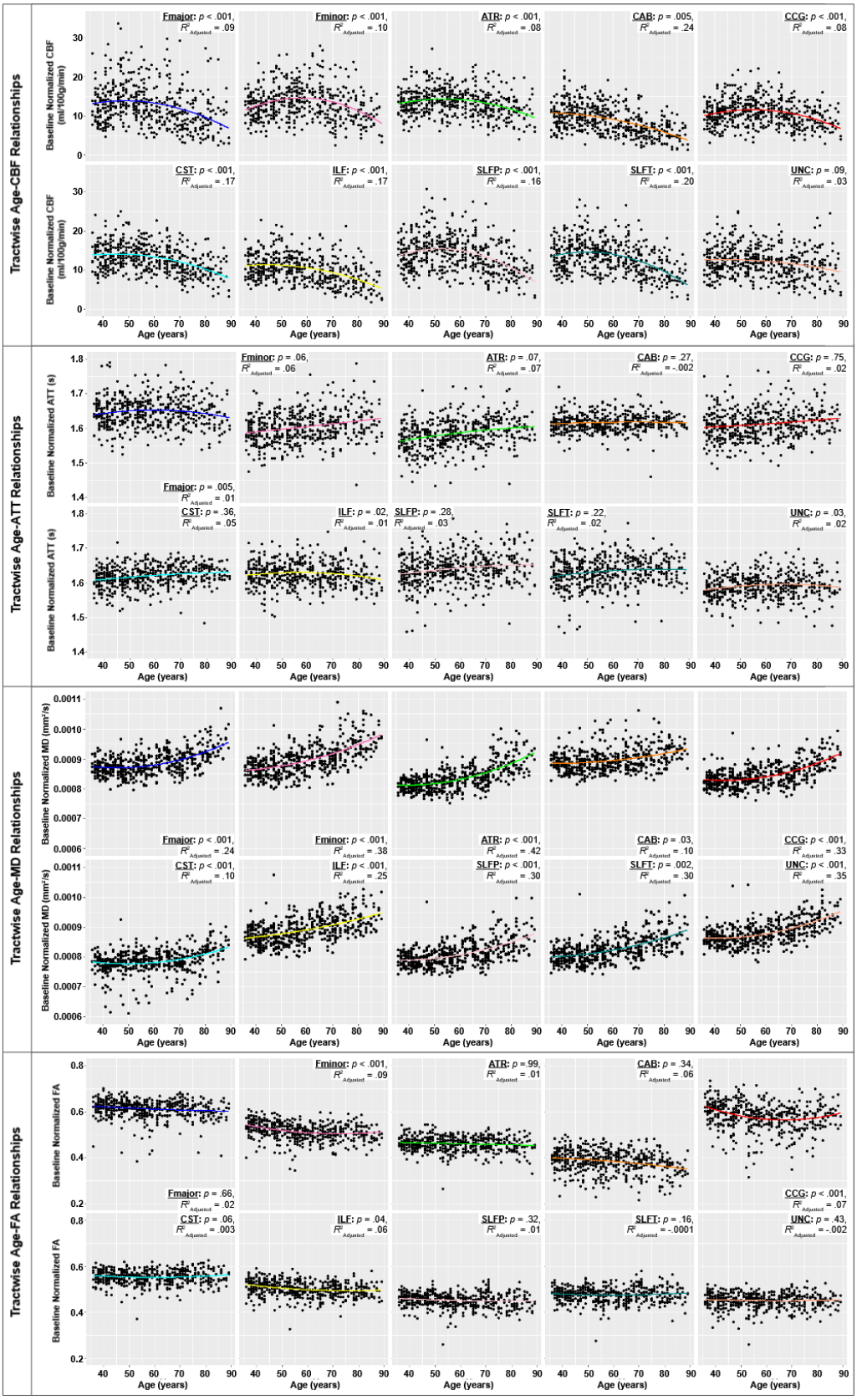

Figure 3: Tractwise quadratic regression of age effects on baseline normalized CBF, ATT, MD, and FA

Sex differences

Female subjects showed significantly higher $MD_{percent}$ in the Fmajor, ATR, CST, ILF, SLFP, and SLFT in regression analysis. While female subjects also demonstrated higher $FA_{percent}$ in the Fmajor, male subjects showed higher $FA_{percent}$ in the Fminor, CCG, SLFP, and SLFT. Female subjects demonstrated higher $CBF_{percent}$ in the CAB, while male subjects showed higher $CBF_{percent}$ in the ATR. Female subjects showed higher $ATT_{percent}$ in the SLFP and SLFT, while male subjects showed higher $ATT_{percent}$ in the ILF (Figure 4).

Tractwise Sex Differences in Baseline Normalized Microstructural/Perfusion Measures (Covaried for Age)
Significant differences are colored. Red: Female>Male. Blue: Male>Female.

Tract	CBF	ATT	MD	FA
Fmajor				
Fminor				
ATR				
CAB				
CCG				
CST				
ILF				
SLFP				
SLFT				
UNC				

Figure 4: Tractwise sex differences in baseline normalized CBF, ATT, MD, and FA

Microstructure-perfusion relationships

Model 1 (perfusion vs microstructure): Significant negative relationships were found between tractwise $CBF_{percent}$ and $MD_{percent}$ in the ILF and SLFT. Significant positive relationships between $ATT_{percent}$ and $MD_{percent}$ were identified in the Fminor, ATR, SLFP, and SLFT. A single significant positive association was found between $CBF_{percent}$ and $FA_{percent}$ in the CCG. A significant negative relationship between $ATT_{percent}$ and $FA_{percent}$ was identified in the ATR, along with a positive relationship in the CAB (Table 1b).

Model 2 (sex differences in perfusion-microstructure relationships): After dividing the sample by sex, significant positive associations were found between $CBF_{percent}$ and $FA_{percent}$ in the CCG in both female and male subjects, as well as in the ATR in female subjects alone. A single negative association between $CBF_{percent}$ and $FA_{percent}$ was found in the CST in male subjects. Female subjects also demonstrated both a negative association between $ATT_{percent}$ and $FA_{percent}$ in the ATR, and a positive association between $ATT_{percent}$ and $FA_{percent}$ in the CAB. No associations were identified between perfusion and MD after dividing the sample by sex (Table 2b).

CCA

Cross correlation analysis identified multiple patterns of association between microstructure and perfusion loadings in male and female subjects. Loadings are listed for significant canonical correlations using a threshold of 0.5. In female subjects, $CBF_{percent}$ contributed significantly eight tracts, while $ATT_{percent}$ contributed significantly in seven. $AD_{percent}$, $RD_{percent}$, and $FA_{percent}$ loaded significantly in five, six, and one tract respectively. In male subjects, $CBF_{percent}$ loaded significantly in four tracts, while $ATT_{percent}$ loaded significantly in three. Male microstructural contributions showed significant loading by $AD_{percent}$ in two tracts, $RD_{percent}$ in two tracts, and $FA_{percent}$ in two tracts (Figure 5).

Tracts were clustered in two categories. Category (i) was defined by tracts demonstrating significant CBF and AD contributions loading in opposite directions with negligible RD loading, suggesting early stages of degeneration, while category (ii) was defined by opposing CBF and RD loading with matched or negligible AD contributions, suggesting more advanced degeneration. Two tracts exhibited pattern (i) in female subjects (ATR, SLFT), along with five in pattern (ii) (Fminor, CCG, CST, ILF, UNC). In male subjects, Two tracts exhibited pattern (i) (CAB, SLFT) with two tracts exhibiting pattern (ii) (ATR, CST).

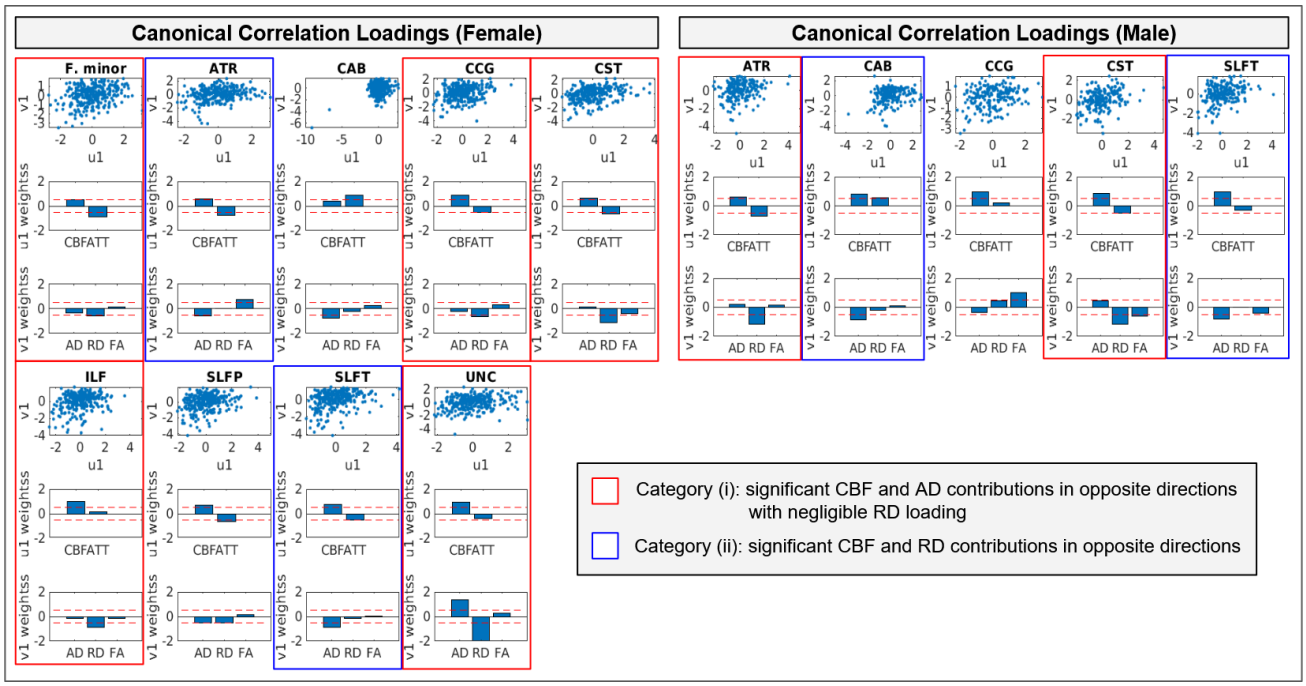

Figure 5: Tractwise contributions by perfusion (CBF/ATT) and microstructural (AD/RD/FA) measures to categorical perfusion-microstructure relationships divided by sex.

CCF

At zero lag, significant correlations between $CBF_{percent}$ and $FA_{percent}$ were identified in the Fmajor, CAB, CCG, CST, and SLFT, along with correlations at positive lag in the SLFP and UNC, such that $FA_{percent}$ led $CBF_{percent}$. Significant zero-lag correlations were identified between $CBF_{percent}$ and both $AD_{percent}$ and $RD_{percent}$ in all tracts but the Fminor, in which correlations at negative lag were identified for both microstructural measures such that $CBF_{percent}$ led $AD_{percent}$/$RD_{percent}$. A single significant zero-lag correlation was found between $ATT_{percent}$ and $FA_{percent}$ in the SLFT, along with a correlation at negative lag in the UNC. Significant zero-lag correlations were found between $ATT_{percent}$ and $AD_{percent}$ in the Fmajor, CST, and SLFP, along with a correlation at negative lag in the UNC. A single significant zero-lag correlation was found between $ATT_{percent}$ and $RD_{percent}$ in the ILF, along with significant correlations at negative lag in the Fmajor, SLFT, and UNC.

Comparisons between $AD_{percent}$ and $RD_{percent}$ round significant zero-lag correlations in all tracts, while comparisons between $FA_{percent}$ and both $AD_{percent}$ and $RD_{percent}$ found zero-lag correlations in the Fmajor, CCG, CST, SLFP, and UNC for both measures, along with significant correlations at negative lag in the SLFT. Comparisons between $CBF_{percent}$ and $ATT_{percent}$ found zero-lag correlations in the Fmajor, ILF, SLFT, and UNC.

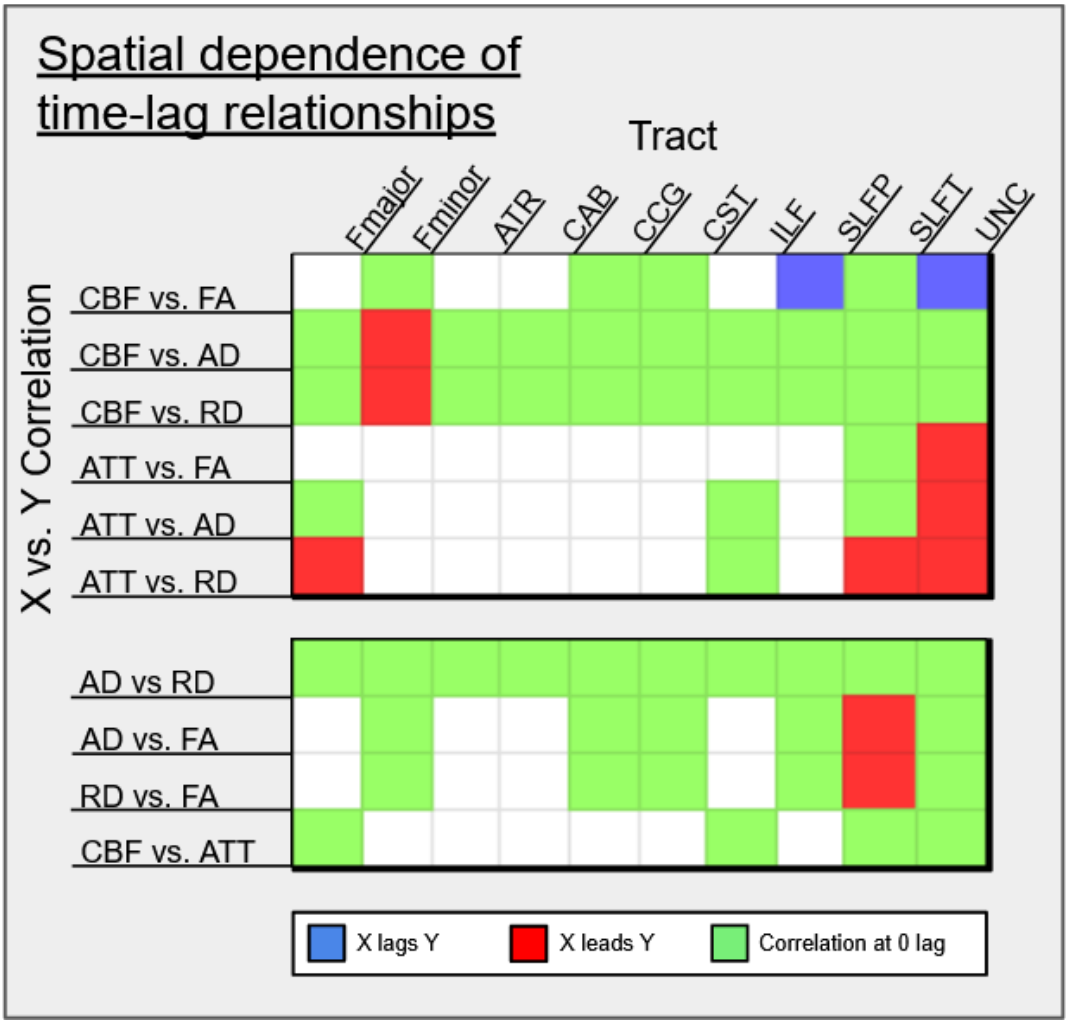

Figure 6: Tractwise cross-correlation results demonstrating significant correlations at positive, negative and zero lag by age category.

DISCUSSION

We initially hypothesized that (1) tractwise microstructural and perfusion declines would not progress at the same rate in aging due to (2) earlier detectable declines in WM perfusion than microstructural integrity. Our findings support hypothesis 1, but also highlight the fact that the patterns of decline were much more varied both by tract and by measure than initially expected.

In addition to the well-established MD and FA associations with age, we also found significant and consistent CBF associations with WM microstructural integrity. Specifically, CBF declines with advancing age in the vast majority of WM tracts, mirroring the age-associated increases in tractwise MD (Figure 3). CBF appears to demonstrate a peak in middle-age, with the peak point varying by tract.

However, FA was not uniformly associated with age across tracts, indicating variability in patterns or rates of WM decline. Moreover, these trajectories of perfusion and microstructural declines vary considerably by tract, with some demonstrating distinct quadratic patterns, and others indicating more linear declines.

Comparison between perfusion and microstructural declines saw wide variation in rates between the tracts examined in the study. Furthermore, the interrelation between perfusion and microstructural integrity was similarly varied. This suggests that the relationships between measures of microstructure and perfusion vary along the course of WM degeneration, highlighting the importance of investigating the origins of this disparity across multiple imaging modalities. Moreover, rather than a smooth shared trajectory of decline, our evidence indicates the presence of stages of a much more complex array of cellular breakdown as it relates to changes in diffusion through axonal fibers. Our findings appear to indicate two probable stages captured in our sample: a relatively early stage (i) marked by impaired axonal diffusion and a later stage (ii) marked by progressive demyelination of axon fibers.

In stage (i), variations in perfusion are accompanied by variations in AD in aging, potentially due to the deterioration of crossing fibers affecting diffusivity prior to fiber breakdown in the tract in question (Uddin et al., 2019). In our data, this is marked by significant and opposing loading by CBF and AD (Figure 5). In stage (ii), significant CBF contributions are accompanied by opposing RD contributions, with or without the presence of AD loading. In this stage, we speculate that myelin breakdown in the tested fiber bundle and the culling of vulnerable axons indicative of advancing degeneration has resulted in an increasing degree of diffusion through the fiber bundle. Across sexes, our results appear to indicate that fronto-inferior tracts decline at a relatively higher rate than those in the posterior WM. This appears consistent with existing anterior-posterior retrogenesis hypotheses (Hoagey et al., 2019; Slater et al., 2019), though the validity of this support remains to be tested. A notable exception to this is the CST, a tract presumed to survive relatively robustly into later age (Michielse et al., 2010) that falls into category (ii) in our CCA results. As the CST does exhibit the lowest MD increases and no significant differences in FA with age, there may be additional factors involved in maintaining this microstructural integrity despite perfusion declines. As axon diameter comparisons across the WM have observed relatively high mean diameter in CST fibers (Liewald et al., 2014), this may suggest that fiber diameter in healthy WM is the key predictor for resilience to perfusion declines.

As these different signatures of perfusion-microstructure association potentially represent different stages of an assumedly common sequence of decline, there is also the likelihood that some tracts remain at intermediate stages of degeneration for longer or shorter periods of time relative to one another. The threshold of perfusion declines necessary for a fiber tract to tip from one signature of microstructural decline into the next may vary due to untested factors, either microstructural: such as the aforementioned

mean axon diameter differences, or microvascular: such as regional differences in number of vascular sources. As myelination represents one of, if not the most significant factor in maintaining WM integrity with age (Hase et al., 2018; Kohama et al., 2012; Tang et al., 1997), differences in myelination trajectory and the ages at which regions fully myelinate may also play a part in determining regional robustness to perfusion changes. Additionally, our findings may reflect differing metabolic sensitivity to perfusion declines, as differing metabolic demands have been observed between larger and smaller fibers (Harris & Attwell, 2012).

While perfusion-microstructure associations differed by tract, these same associations varied considerably between sexes. Overall, female subjects demonstrated but a greater number of tracts with significant relationships between WM microstructure and perfusion, as well as proportionally more tracts in category (ii), suggesting a relatively more advanced state of decline in WM across the brain. This finding is consistent with previous reports (Intzandt et al., 2023; Patel et al., 2023). We speculate that a likely cause of these differences in WM aging by sex are the effects of menopause on brain health more broadly. Menopause has previously been found to affect structural, connectivity, and metabolic measures in the brain (Mosconi et al., 2021). Notably, cognitive impacts appear to stabilize post-menopause, though this is speculated to be the result of compensatory effects, rather than improvement in structural integrity. The sex differences with age observed in this study likely capture structural and microvascular impacts of peri- and postmenopause on the WM, though direct associations between these declines and cognitive performance will require additional investigation. Should microvascular declines be associated with cognitive performance similarly to the microstructural associations identified in this study, targeting vascular declines may benefit the study of interventions in the impacts of menopause on the brain in addition to the aging brain more generally. The degree to which hormone supplementation therapies may mitigate these effects, and indeed the mechanisms of estrogen's effects on WM health more generally, will require further investigation.

Furthermore, while FA draws considerable attention in aging research as a measure of microstructural integrity, our findings suggest that it contributes less to microstructural-perfusion interactions in aging than AD or RD. Even prior to examining tractwise variation across the brain, these results raise questions regarding established approaches to assessing WM declines with age and the reliance of many studies on FA as a measure of microstructural decline. Our results may indicate that other measures of microstructural decline are more sensitive to early changes in the WM.

The results of our cross-correlation analysis indicate that ATT may indeed precede microstructural declines in certain tracts. CBF, in contrast, appears to decline contemporaneously with microstructure. The superior sensitivity of vascular timing information to pathology is consistent with recent reports on the unique sensitivity of vascular-response latency (D. Kim et al., 2021; McKetton et al.,

2019; Nanayakkara et al., 2023). A notable limitation to these findings is that, while CBF declined quadratically in all tracts by the UNC, the predominantly linear declines in ATT restricted the extent of possible CCF comparisons. This raises the question of whether the age lagged effects found in the Fmajor, SLFT, and UNC can be taken as representative of WM declines more generally, or if this early detection on the part of ATT is unique to these tracts. As the Fminor demonstrated CBF declines leading microstructural declines despite contemporaneous declines between CBF and AD/RD in other tracts, the age at which these changes are detectable may also vary by tract. Clarifying age lagged relationships in those tracts exhibiting linear declines will require either a wider age sample able to capture younger peak ATT values, or analysis of longitudinal data. Nonetheless, this is the first time that perfusion has been directly demonstrated as an earlier indicator of WM decline than microstructure. Incorporating ATT, in addition to a more nuanced modeling of diffusion changes, may be necessary for similar investigations in future as we theorize that CBF and ATT reflect different, equally informative aspects of vascular aging.

Conclusions

Relationships between age, perfusion, and microstructural integrity assessed in this study depict highly tract-specific, as well as sex-specific, variation across our sample. The lack of a unified set of trends between perfusion and microstructural declines across tracts supports our hypothesis that WM perfusion and microstructure do not decline at the same rate in aging. Additionally, our secondary hypothesis that WM perfusion differences would be detectable earlier than differences in microstructural integrity, found limited support in evidence that tractwise age effect on ATT anticipate age effects in multiple microstructural measures. However, the ubiquity of CBF as a significant component in contemporaneous perfusion-microstructure relationships demonstrates that perfusion changes in the WM are complex and warrant greater attention in aging research. To our knowledge, this study is the first demonstration of tractwise declines in WM CBF and ATT with age, and these findings will be highly valuable to the development of a more unified model for mechanisms of brain aging.

References

Akashi, T., Takahashi, S., Mugikura, S., Sato, S., Murata, T., Umetsu, A., & Takase, K. (2017). Ischemic White Matter Lesions Associated With Medullary Arteries: Classification of MRI Findings Based on the Anatomic Arterial Distributions. *AJR. American Journal of Roentgenology*, *209*(3), W160–W168.

Baker, L. M., Laidlaw, D. H., Conturo, T. E., Hogan, J., Zhao, Y., Luo, X., Correia, S., Cabeen, R., Lane, E. M., Heaps, J. M., Bolzenius, J., Salminen, L. E., Akbudak, E., McMichael, A. R., Usher, C., Behrman, A., & Paul, R. H. (2014). White matter changes with age utilizing quantitative diffusion MRI. *Neurology*, *83*(3), 247–252.

Bender, A. R., Völkle, M. C., & Raz, N. (2016). Differential aging of cerebral white matter in middle-aged and older adults: A seven-year follow-up. *NeuroImage*, *125*, 74–83.

Bernbaum, M., Menon, B. K., Fick, G., Smith, E. E., Goyal, M., Frayne, R., & Coutts, S. B. (2015). Reduced blood flow in normal white matter predicts development of leukoaraiosis. *Journal of Cerebral Blood Flow and Metabolism: Official Journal of the International Society of Cerebral Blood Flow and Metabolism*, *35*(10), 1610–1615.

Bookheimer, S. Y., Salat, D. H., Terpstra, M., Ances, B. M., Barch, D. M., Buckner, R. L., Burgess, G. C., Curtiss, S. W., Diaz-Santos, M., Elam, J. S., Fischl, B., Greve, D. N., Hagy, H. A., Harms, M. P., Hatch, O. M., Hedden, T., Hodge, C., Japardi, K. C., Kuhn, T. P., … Yacoub, E. (2019). The Lifespan Human Connectome Project in Aging: An overview. *NeuroImage*, *185*, 335–348.

Chen, J. J., Rosas, H. D., & Salat, D. H. (2011). Age-associated reductions in cerebral blood flow are independent from regional atrophy. *NeuroImage*, *55*(2), 468–478.

Chen, J. J., Rosas, H. D., & Salat, D. H. (2013). The relationship between cortical blood flow and sub-cortical white-matter health across the adult age span. *PloS One*, *8*(2), e56733.

de Groot, M., Cremers, L. G. M., Ikram, M. A., Hofman, A., Krestin, G. P., van der Lugt, A., Niessen, W. J., & Vernooij, M. W. (2016). White Matter Degeneration with Aging: Longitudinal Diffusion MR

Imaging Analysis. *Radiology*, *279*(2), 532–541.

de Groot, M., Ikram, M. A., Akoudad, S., Krestin, G. P., Hofman, A., van der Lugt, A., Niessen, W. J., & Vernooij, M. W. (2015). Tract-specific white matter degeneration in aging: the Rotterdam Study. *Alzheimer's & Dementia: The Journal of the Alzheimer's Association*, *11*(3), 321–330.

Harms, M. P., Somerville, L. H., Ances, B. M., Andersson, J., Barch, D. M., Bastiani, M., Bookheimer, S. Y., Brown, T. B., Buckner, R. L., Burgess, G. C., Coalson, T. S., Chappell, M. A., Dapretto, M., Douaud, G., Fischl, B., Glasser, M. F., Greve, D. N., Hodge, C., Jamison, K. W., … Yacoub, E. (2018). Extending the Human Connectome Project across ages: Imaging protocols for the Lifespan Development and Aging projects. *NeuroImage*, *183*, 972–984.

Harris, J. J., & Attwell, D. (2012). The energetics of CNS white matter. *The Journal of Neuroscience: The Official Journal of the Society for Neuroscience*, *32*(1), 356–371.

Hase, Y., Horsburgh, K., Ihara, M., & Kalaria, R. N. (2018). White matter degeneration in vascular and other ageing-related dementias. *Journal of Neurochemistry*, *144*(5), 617–633.

Hoagey, D. A., Rieck, J. R., Rodrigue, K. M., & Kennedy, K. M. (2019). Joint contributions of cortical morphometry and white matter microstructure in healthy brain aging: A partial least squares correlation analysis. *Human Brain Mapping*, *40*(18), 5315–5329.

Intzandt, B., Sanami, S., Huck, J., PREVENT-AD Research group, Villeneuve, S., Bherer, L., & Gauthier, C. J. (2023). Sex-specific relationships between obesity, physical activity, and gray and white matter volume in cognitively unimpaired older adults. *GeroScience*. https://doi.org/10.1007/s11357-023-00734-4

Kim, C.-M., Alvarado, R. L., Stephens, K., Wey, H.-Y., Wang, D. J. J., Leritz, E. C., & Salat, D. H. (2020). Associations between cerebral blood flow and structural and functional brain imaging measures in individuals with neuropsychologically defined mild cognitive impairment. *Neurobiology of Aging*, *86*, 64–74.

Kim, D., Hughes, T. M., Lipford, M. E., Craft, S., Baker, L. D., Lockhart, S. N., Whitlow, C. T., Okonmah-Obazee, S. E., Hugenschmidt, C. E., Bobinski, M., & Jung, Y. (2021). Relationship

Between Cerebrovascular Reactivity and Cognition Among People With Risk of Cognitive Decline. *Frontiers in Physiology*, *12*, 645342.

Kobayashi, K., Hayashi, M., Nakano, H., Fukutani, Y., Sasaki, K., Shimazaki, M., & Koshino, Y. (2002). Apoptosis of astrocytes with enhanced lysosomal activity and oligodendrocytes in white matter lesions in Alzheimer's disease. *Neuropathology and Applied Neurobiology*, *28*(3), 238–251.

Kohama, S. G., Rosene, D. L., & Sherman, L. S. (2012). Age-related changes in human and non-human primate white matter: from myelination disturbances to cognitive decline. *Age* , *34*(5), 1093–1110.

Kohn, J. C., Lampi, M. C., & Reinhart-King, C. A. (2015). Age-related vascular stiffening: causes and consequences. *Frontiers in Genetics*, *6*, 112.

Liewald, D., Miller, R., Logothetis, N., Wagner, H.-J., & Schüz, A. (2014). Distribution of axon diameters in cortical white matter: an electron-microscopic study on three human brains and a macaque. *Biological Cybernetics*, *108*(5), 541–557.

Li, Y., Choi, W. J., Wei, W., Song, S., Zhang, Q., Liu, J., & Wang, R. K. (2018). Aging-associated changes in cerebral vasculature and blood flow as determined by quantitative optical coherence tomography angiography. *Neurobiology of Aging*, *70*, 148–159.

Maffei, C., Lee, C., Planich, M., Ramprasad, M., Ravi, N., Trainor, D., Urban, Z., Kim, M., Jones, R. J., Henin, A., Hofmann, S. G., Pizzagalli, D. A., Auerbach, R. P., Gabrieli, J. D. E., Whitfield-Gabrieli, S., Greve, D. N., Haber, S. N., & Yendiki, A. (2021). Using diffusion MRI data acquired with ultra-high gradients to improve tractography in routine-quality data. In *bioRxiv* (p. 2021.06.28.450265). https://doi.org/10.1101/2021.06.28.450265

Mayer, C., Frey, B. M., Schlemm, E., Petersen, M., Engelke, K., Hanning, U., Jagodzinski, A., Borof, K., Fiehler, J., Gerloff, C., Thomalla, G., & Cheng, B. (2021). Linking cortical atrophy to white matter hyperintensities of presumed vascular origin. *Journal of Cerebral Blood Flow and Metabolism: Official Journal of the International Society of Cerebral Blood Flow and Metabolism*, *41*(7), 1682–1691.

McKetton, L., Cohn, M., Tang-Wai, D. F., Sobczyk, O., Duffin, J., Holmes, K. R., Poublanc, J., Sam, K.,

Crawley, A. P., Venkatraghavan, L., Fisher, J. A., & Mikulis, D. J. (2019). Cerebrovascular Resistance in Healthy Aging and Mild Cognitive Impairment. *Frontiers in Aging Neuroscience*, *11*, 79.

Michielse, S., Coupland, N., Camicioli, R., Carter, R., Seres, P., Sabino, J., & Malykhin, N. (2010). Selective effects of aging on brain white matter microstructure: a diffusion tensor imaging tractography study. *NeuroImage*, *52*(4), 1190–1201.

Mosconi, L., Berti, V., Dyke, J., Schelbaum, E., Jett, S., Loughlin, L., Jang, G., Rahman, A., Hristov, H., Pahlajani, S., Andrews, R., Matthews, D., Etingin, O., Ganzer, C., de Leon, M., Isaacson, R., & Brinton, R. D. (2021). Menopause impacts human brain structure, connectivity, energy metabolism, and amyloid-beta deposition. *Scientific Reports*, *11*(1), 10867.

Nanayakkara, N. D., Meusel, L.-A., Anderson, N. D., & Chen, J. J. (2023). Robust estimation of dynamic cerebrovascular reactivity using breath-holding fMRI: application in diabetes and hypertension. In *medRxiv*. https://doi.org/10.1101/2023.05.20.23290209

Nonaka, H., Akima, M., Hatori, T., Nagayama, T., Zhang, Z., & Ihara, F. (2003). Microvasculature of the human cerebral white matter: arteries of the deep white matter. *Neuropathology: Official Journal of the Japanese Society of Neuropathology*, *23*(2), 111–118.

Nozais, V., Forkel, S. J., Foulon, C., Petit, L., & Thiebaut de Schotten, M. (2021). Functionnectome as a framework to analyse the contribution of brain circuits to fMRI. *Communications Biology*, *4*(1), 1035.

O'Sullivan, M., Lythgoe, D. J., Pereira, A. C., Summers, P. E., Jarosz, J. M., Williams, S. C. R., & Markus, H. S. (2002). Patterns of cerebral blood flow reduction in patients with ischemic leukoaraiosis. *Neurology*, *59*(3), 321–326.

Patel, A., Chad, J. A., & Chen, J. J. (2023). Is adiposity associated with white matter microstructural health and intelligence differently in males and females? *Obesity* , *31*(4), 1011–1023.

Robinson, T. D., Sun, Y. L., Chang, P. T. H., & Jean Chen, J. (2023). In search of a unifying theory of white matter aging: tract morphometry-microstructure relationships. In *bioRxiv* (p.

2023.03.14.532658). https://doi.org/10.1101/2023.03.14.532658

Sala, S., Agosta, F., Pagani, E., Copetti, M., Comi, G., & Filippi, M. (2012). Microstructural changes and atrophy in brain white matter tracts with aging. *Neurobiology of Aging*, *33*(3), 488–498.e2.

Slater, D. A., Melie-Garcia, L., Preisig, M., Kherif, F., Lutti, A., & Draganski, B. (2019). Evolution of white matter tract microstructure across the life span. *Human Brain Mapping*, *40*(7), 2252–2268.

Smirnov, M., Destrieux, C., & Maldonado, I. L. (2021). Cerebral white matter vasculature: still uncharted? *Brain: A Journal of Neurology*, *144*(12), 3561–3575.

Stricker, N. H., Schweinsburg, B. C., Delano-Wood, L., Wierenga, C. E., Bangen, K. J., Haaland, K. Y., Frank, L. R., Salmon, D. P., & Bondi, M. W. (2009). Decreased white matter integrity in late-myelinating fiber pathways in Alzheimer's disease supports retrogenesis. *NeuroImage*, *45*(1), 10–16.

Tang, Y., Nyengaard, J. R., Pakkenberg, B., & Gundersen, H. J. (1997). Age-induced white matter changes in the human brain: a stereological investigation. *Neurobiology of Aging*, *18*(6), 609–615.

Tomoto, T., Tarumi, T., & Zhang, R. (2023). Central arterial stiffness, brain white matter hyperintensity and total brain volume across the adult lifespan. *Journal of Hypertension*, *41*(5), 819–829.

Uddin, M. N., Figley, T. D., Solar, K. G., Shatil, A. S., & Figley, C. R. (2019). Comparisons between multi-component myelin water fraction, T1w/T2w ratio, and diffusion tensor imaging measures in healthy human brain structures. *Scientific Reports*, *9*(1), 2500.

Yeatman, J. D., Wandell, B. A., & Mezer, A. A. (2014). Lifespan maturation and degeneration of human brain white matter. *Nature Communications*, *5*, 4932.

Yendiki, A., Panneck, P., Srinivasan, P., Stevens, A., Zöllei, L., Augustinack, J., Wang, R., Salat, D., Ehrlich, S., Behrens, T., Jbabdi, S., Gollub, R., & Fischl, B. (2011). Automated probabilistic reconstruction of white-matter pathways in health and disease using an atlas of the underlying anatomy. *Frontiers in Neuroinformatics*, *5*, 23.

Tables

Table 1a: Model 1 - Whole-WM MD/FA Relationships with Perfusion (Covaried for Sex).
Significant associations are bolded. Asterisks indicate significance *:p<.05, **:p<.01, ***:p<.001).

	$MD_{percentage}$		**$FA_{percentage}$**	
Tract	$CBF_{percentage}$	$ATT_{percentage}$	$CBF_{percentage}$	$ATT_{percentage}$
All	$F(2, 497) = 5.36$, $p = .005$, $R^2_{Adjusted} = .02$	$F(2, 497) = 4.07$, $p = .02$, $R^2_{Adjusted} = .01$	$F(2, 497) = 0.40$, $p = .67$, $R^2_{Adjusted} = -.002$	$F(2, 497) = 0.02$, $p = .98$, $R^2_{Adjusted} = -.004$
	-0.018508**	**0.231872***	0.0089404	0.0060844

Table 1b: Model 1 - Tractwise MD/FA Relationships with Perfusion (Covaried for Sex).
Significant associations are bolded. Asterisks indicate significance (*:p<.05, **:p<.01, ***:p<.001).

	$MD_{percentage}$		**$FA_{percentage}$**	
Tract	$CBF_{percentage}$	$ATT_{percentage}$	$CBF_{percentage}$	$ATT_{percentage}$
Fmajor	$F(2, 490) = 7.47$, $p < .001$, $R^2_{Adjusted} = .03$	$F(2, 490) = 5.68$, $p = .004$, $R^2_{Adjusted} = .02$	$F(2, 490) = 8.24$, $p < .001$, $R^2_{Adjusted} = .03$	$F(2, 490) = 8.08$, $p < .001$, $R^2_{Adjusted} = .03$
	-0.009599	0.081493	-0.003605	-0.010087
Fminor	$F(2, 490) = 1.52$, $p = .22$, $R^2_{Adjusted} = .002$	$F(2, 490) = 6,48$, $p = .002$, $R^2_{Adjusted} = .02$	$F(2, 490) = 5.49$, $p = .004$, $R^2_{Adjusted} = .02$	$F(2, 490) = 5.53$, $p = .004$, $R^2_{Adjusted} = .02$
	-0.011735	**0.289540****	0.019804	-0.227797
ATR	$F(2, 494) = 2.08$, $p = .13$, $R^2_{Adjusted} = .004$	$F(2, 494) = 9.13$, $p < .001$, $R^2_{Adjusted} = .03$	$F(2, 494) = 3.23$, $p = .009$, $R^2_{Adjusted} = .04$	$F(2, 494) = 4.22$, $p = .015$, $R^2_{Adjusted} = .01$
	-0.014611	**0.324941*****	0.027963	**-0.306558****
CAB	$F(2, 487) = 0.47$, $p = .62$, $R^2_{Adjusted} = -.002$	$F(2, 487) = 2.69$, $p = .07$, $R^2_{Adjusted} = .007$	$F(2, 487) = 0.75$, $p = .47$, $R^2_{Adjusted} = -.001$	$F(2, 487) = 4.53$, $p = .01$, $R^2_{Adjusted} = .01$

	0.0006211	-0.202510	0.01026	**0.79903***
CCG	$F(2, 492) = 2.48$, $p = .085$, $R^2_{Adjusted} = .006$	$F(2, 492) = 4.82$, $p = .008$, $R^2_{Adjusted} = .02$	$F(2, 492) = 13.3$, $p < .001$, $R^2_{Adjusted} = .05$	$F(2, 492) = 2.60$, $p = .006$, $R^2_{Adjusted} = .08$
	-0.013649	**0.216401****	**0.068524*****	0.050215
CST	$F(2, 488) = 6.42$, $p = .002$, $R^2_{Adjusted} = .02$	$F(2, 488) = 6.19$, $p = .002$, $R^2_{Adjusted} = .02$	$F(2, 488) = 1.89$, $p = .15$, $R^2_{Adjusted} = .004$	$F(2, 488) = 1.80$, $p = .17$, $R^2_{Adjusted} = .003$
	-0.006782	0.050971	-0.018407	0.225689
ILF	$F(2, 494) = 8.03$, $p < .001$, $R^2_{Adjusted} = .03$	$F(2, 494) = 3.67$, $p = .026$, $R^2_{Adjusted} = .01$	$F(2, 494) = 2.28$, $p = .10$, $R^2_{Adjusted} = .005$	$F(2, 494) = 2.90$, $p = .06$, $R^2_{Adjusted} = .008$
	-0.019481*	-0.032828	0.004481	0.16351
SLFP	$F(2, 494) = 3.64$, $p = .027$, $R^2_{Adjusted} = .01$	$F(2, 494) = 5.51$, $p = .004$, $R^2_{Adjusted} = .02$	$F(2, 494) = 2.15$, $p = .12$, $R^2_{Adjusted} = .005$	$F(2, 494) = 4.46$, $p = .012$, $R^2_{Adjusted} = .01$
	-0.014721	**0.214620***	-0.007393	-0.247955
SLFT	$F(2, 492) = 5.01$, $p = .007$, $R^2_{Adjusted} = .02$	$F(2, 492) = 7.78$, $p = .008$, $R^2_{Adjusted} = .02$	$F(2, 492) = 4.99$, $p = .007$, $R^2_{Adjusted} = .02$	$F(2, 492) = 3.37$, $p = .035$, $R^2_{Adjusted} = .009$
	-0.021370*	**0.222030***	-0.021391	-0.127256
UNC	$F(2, 492) = 0.49$, $p = .61$, $R^2_{Adjusted} = -.002$	$F(2, 492) = 0.82$, $p = .44$, $R^2_{Adjusted} = -.0007$	$F(2, 492) = 5.06$, $p = .007$, $R^2_{Adjusted} = .02$	$F(2, 492) = 4.33$, $p = .014$, $R^2_{Adjusted} = .01$
	-0.0055602	0.1058895	0.015398	-0.143507

Table 2a: Model 2 - While-WM Sex Differences in Relationships Between MD/FA and Perfusion (Covaried for Age).
Significant associations are bolded. Asterisks indicate significance (*:p<.05, **:p<.01, ***:p<.001).

	$MD_{percentage}$				**$FA_{percentage}$**			
	$CBF_{percentage}$		$ATT_{percentage}$		CBF		ATT	
Tract	Female	Male	Female	Male	Female	Male	Female	Male
All	$F(2, 291) = 55.5$, $p < .001$, $R^2_{Adjusted} = .27$	$F(2, 203) = 33.2$, $p < .001$, $R^2_{Adjusted} = .17$	$F(2, 291) = 55.1$, $p < .001$, $R^2_{Adjusted} = .27$	$F(2, 203) = 22.3$, $p < .001$, $R^2_{Adjusted} = .17$	$F(2, 291) = 9.72$, $p < .001$, $R^2_{Adjusted} = .06$	$F(2, 203) = 1.86$, $p = .16$, $R^2_{Adjusted} = .008$	$F(2, 291) = 9.51$, $p < .001$, $R^2_{Adjusted} = .05$	$F(2, 203) = 1.60$, $p = .20$, $R^2_{Adjusted} = .006$
	-0.0079527	-0.0007841	0.0559703	-0.0668848	0.0130418	-0.0143295	0.1261818	0.1857851

Table 2b: Model 2 - Tractwise Sex Differences in Relationships Between MD/FA and Perfusion (Covaried for Age).
Significant associations are bolded. Asterisks indicate significance (*:p<.05, **:p<.01, ***:p<.001).

	$MD_{percentage}$				**$FA_{percentage}$**			
	$CBF_{percentage}$		$ATT_{percentage}$		$CBF_{percentage}$		$ATT_{percentage}$	
Tract	Female	Male	Female	Male	Female	Male	Female	Male
Fmajor	$F(2, 287) = 31.3$, $p < .001$, $R^2_{Adjusted} = .17$	$F(2, 200) = 9.30$, $p < .001$, $R^2_{Adjusted} = .009$	$F(2, 287) = 32.9$, $p < .001$, $R^2_{Adjusted} = .18$	$F(2, 200) = 8.95$, $p < .001$, $R^2_{Adjusted} = .07$	$F(2, 287) = 3.44$, $p = .034$, $R^2_{Adjusted} = .02$	$F(2, 200) = 1.96$, $p = .14$, $R^2_{Adjusted} = .009$	$F(2, 287) = 2.92$, $p = .056$, $R^2_{Adjusted} = .01$	$F(2, 200) = 1.96$, $p = .14$, $R^2_{Adjusted} = .009$
	-0.0039667	-0.0076777	0.1285074	0.0116263	-0.0093200	-0.0026277	-0.0444465	0.0518249
Fminor	$F(2, 288) = 77.5$, $p < .001$, $R^2_{Adjusted} = .35$	$F(2, 199) = 26.6$, $p < .001$, $R^2_{Adjusted} = .20$	$F(2, 288) = 76.8$, $p < .001$, $R^2_{Adjusted} = .34$	$F(2, 199) = 26.7$, $p < .001$, $R^2_{Adjusted} = .20$	$F(2, 288) = 24.4$, $p < .001$, $R^2_{Adjusted} = .14$	$F(2, 199) = 10.6$, $p < .001$, $R^2_{Adjusted} = .09$	$F(2, 288) = 22.0$, $p < .001$, $R^2_{Adjusted} = .13$	$F(2, 199) = 10.6$, $p < .001$, $R^2_{Adjusted} = .09$
	-0.0093523	-0.0011248	0.0490044	0.0443195	0.0248039	0.0045800	-0.0178029	-0.061765

ATR	$F(2, 289) = 63.6$, $p < .001$, $R^2_{Adjusted} = .30$	$F(2, 202) = 32.7$, $p < .001$, $R^2_{Adjusted} = .24$	$F(2, 289) = 65.0$, $p < .001$, $R^2_{Adjusted} = .31$	$F(2, 202) = 32.3$, $p < .001$, $R^2_{Adjusted} = .23$	$F(2, 289) = 8.25$, $p < .001$, $R^2_{Adjusted} = .05$	$F(2, 202) = 0.25$, $p = .78$, $R^2_{Adjusted} = -.007$	$F(2, 289) = 8.44$, $p < .001$, $R^2_{Adjusted} = .05$	$F(2, 202) = 0.08$, $p = .92$, $R^2_{Adjusted} = -.009$
	-0.0023397	-0.0075814	0.1296512	-0.0436909	**0.0427019***	0.0094317	**-0.3579011***	-0.0112258
CAB	$F(2, 285) = 14.5$, $p < .001$, $R^2_{Adjusted} = .09$	$F(2, 199) = 2.56$, $p = .08$, $R^2_{Adjusted} = .02$	$F(2, 285) = 14.3$, $p < .001$, $R^2_{Adjusted} = .08$	$F(2, 199) = 4.17$, $p = .016$, $R^2_{Adjusted} = .03$	$F(2, 285) = 7.74$, $p < .001$, $R^2_{Adjusted} = .04$	$F(2, 199) = 4.04$, $p = .02$, $R^2_{Adjusted} = .03$	$F(2, 285) = 11.2$, $p < .001$, $R^2_{Adjusted} = .07$	$F(2, 199) = 4.68$, $p = .01$, $R^2_{Adjusted} = .04$
	0.0114287	0.0064030	-0.1455464	-0.3302063	-0.0086050	-0.0161303	**0.7990257***	0.7374741
CCG	$F(2, 289) = 41.1$, $p < .001$, $R^2_{Adjusted} = .22$	$F(2, 200) = 18.6$, $p < .001$, $R^2_{Adjusted} = .15$	$F(2, 289) = 42.5$, $p < .001$, $R^2_{Adjusted} = .22$	$F(2, 200) = 18.4$, $p < .001$, $R^2_{Adjusted} = .15$	$F(2, 289) = 17.9$, $p < .001$, $R^2_{Adjusted} = .10$	$F(2, 200) = 11.5$, $p < .001$, $R^2_{Adjusted} = .09$	$F(2, 289) = 14.8$, $p < .001$, $R^2_{Adjusted} = .09$	$F(2, 200) = 6.26$, $p = .002$, $R^2_{Adjusted} = .05$
	-0.010615	-0.0046832	0.1605160	-0.0354249	**0.0482986***	**0.0755159*****	0.107982	0.5138831
CST	$F(2, 284) = 9.29$, $p < .001$, $R^2_{Adjusted} = .05$	$F(2, 201) = 1.37$, $p = .26$, $R^2_{Adjusted} = .004$	$F(2, 284) = 9.60$, $p < .001$, $R^2_{Adjusted} = .06$	$F(2, 201) = 1.35$, $p = .26$, $R^2_{Adjusted} = .003$	$F(2, 284) = 0.97$, $p = .38$, $R^2_{Adjusted} = -.0002$	$F(2, 201) = 3.67$, $p = .03$, $R^2_{Adjusted} = .03$	$F(2, 284) = 1.97$, $p = .14$, $R^2_{Adjusted} = .007$	$F(2, 201) = 1.29$, $p = .28$, $R^2_{Adjusted} = .003$
	0.0061903	-0.0065296	-0.1043070	0.0842141	-0.0054017	**-0.03705****	0.2295747	0.3193
ILF	$F(2, 289) = 43.0$, $p < .001$, $R^2_{Adjusted} = .22$	$F(2, 202) = 17.7$, $p < .001$, $R^2_{Adjusted} = .14$	$F(2, 289) = 41.8$, $p < .001$, $R^2_{Adjusted} = .22$	$F(2, 202) = 17.7$, $p < .001$, $R^2_{Adjusted} = .14$	$F(2, 289) = 10.3$, $p < .001$, $R^2_{Adjusted} = .06$	$F(2, 202) = 3.82$, $p = .02$, $R^2_{Adjusted} = .03$	$F(2, 289) = 10.7$, $p < .001$, $R^2_{Adjusted} = .06$	$F(2, 202) = 3.50$, $p = .03$, $R^2_{Adjusted} = .02$
	-0.0125893	0.0018092	0.0240348	0.0051664	-0.0020199	-0.0112217	0.1423583	0.0884416
SLFP	$F(2, 288) = 47.8$, $p < .001$, $R^2_{Adjusted} = .24$	$F(2, 203) = 20.6$, $p < .001$, $R^2_{Adjusted} = .16$	$F(2, 288) = 48.1$, $p < .001$, $R^2_{Adjusted} = .25$	$F(2, 203) = 20.8$, $p < .001$, $R^2_{Adjusted} = .16$	$F(2, 288) = 7.54$, $p < .001$, $R^2_{Adjusted} = .04$	$F(2, 203) = 1.73$, $p = .18$, $R^2_{Adjusted} = .007$	$F(2, 288) = 8,76$, $p < .001$, $R^2_{Adjusted} = .05$	$F(2, 203) = 0.41$, $p = .67$, $R^2_{Adjusted} = -.006$
	-0.0059281	0.0023829	0.0836243	0.0632643	-0.00005828	-0.02840	-0.2094319	-0.1595419

SLFT	$F(2, 287) = 52.9$, $p < .001$, $R^2_{Adjusted} = .26$	$F(2, 202) = 22.2$, $p < .001$, $R^2_{Adjusted} = .17$	$F(2, 287) = 53.6$, $p < .001$, $R^2_{Adjusted} = .27$	$F(2, 202) = 22.3$, $p < .001$, $R^2_{Adjusted} = .17$	$F(2, 287) = 4.30$, $p = .014$, $R^2_{Adjusted} = .02$	$F(2, 202) = 6.02$, $p = .003$, $R^2_{Adjusted} = .05$	$F(2, 287) = 4.59$, $p = .011$, $R^2_{Adjusted} = .02$	$F(2, 202) = 1.80$, $p = .17$, $R^2_{Adjusted} = .008$
	-0.0078787	0.0006048	0.1188965	0.0478854	-0.0097048	**-0.0440165****	-0.1308776	-0.0510914
UNC	$F(2, 290) = 49.5$, $p < .001$, $R^2_{Adjusted} = .25$	$F(2, 199) = 18.4$, $p < .001$, $R^2_{Adjusted} = .15$	$F(2, 290) = 49.8$ $p < .001$, $R^2_{Adjusted} = .25$	$F(2, 199) = 18.4$, $p < .001$, $R^2_{Adjusted} = .15$	$F(2, 290) = 3.21$, $p = .04$, $R^2_{Adjusted} = .01$	$F(2, 199) = 0.30$, $p = .74$, $R^2_{Adjusted} = -.007$	$F(2, 290) = 1.28$, $p = .28$, $R^2_{Adjusted} = .002$	$F(2, 199) = 0.32$, $p = .73$, $R^2_{Adjusted} = -.007$
	0.00004331	0.0009167	0.0632672	-0.0315701	0.0289662	-0.0053114	-0.1422849	-0.0935715